

<http://ansinet.com/itj>

ITJ

ISSN 1812-5638

# INFORMATION TECHNOLOGY JOURNAL

**ANSI***net*

Asian Network for Scientific Information  
308 Lasani Town, Sargodha Road, Faisalabad - Pakistan



camera lens is  $u_0$  and the distances from camera plane to camera lens is  $v_0$ , we can obtain a clear image. If changes the distances from camera plane to camera lens, a blur image can be seen in CCD camera plane. When keeps a constant for camera parameter, it can be given the relationship between image defocus radius and the depth of image as shown in Eq. (2):

$$u = \frac{fv_0}{v_0 - f - Fr_b} \quad (2)$$

For Eq. (2),  $F$  is the  $F$  number of CCD lens.  $r_b$  is the defocus radius of image and  $u$  is the depth of the image. Therefore, there is a corresponding function relationship between the distances from CCD lens to object and the defocus radius of blur image, which can be used to obtain the depth of the image. According to Eq. (2), the positive or negative of distances  $u$  depends on if the focus image locates fore or back in image plane. We restrict that the distances of object is higher than the distances of image. The Eq. (2) can be converted into Eq. (3):

$$r_b = \frac{fv_0}{F} \left( \frac{1}{f} - \frac{1}{v_0} - \frac{1}{u} \right) \quad (3)$$

For two captured image with different focus length setting, we have Eq. (4):

$$r_b^i = \frac{f_i v_i}{F} \left( \frac{1}{f_i} - \frac{1}{v_i} - \frac{1}{u} \right) \quad i=1,2 \quad (4)$$

For defocus image, the blur parameter is  $\rho$  and is given by  $\rho = \beta r_b$ . With giving value  $i = 1, 2$  and eliminating  $u$ , the relationship of two defocus image's blur parameter is shown as Eq. (5):

$$\rho^j = m\rho^2 + n \quad (5)$$

Since the blur parameter  $\rho^j$  at location  $(x, y)$  is related to the depth of the scene, we can construct a model of the blue parameter based on MRF, meaning that the depth of the scene can be obtained indirectly.

### CONSTRUCTING THE BLUR PARAMETER MODEL BASED MRF

**MRF and Gibbs distribution:** For image function  $X$  in 2D image plane, it is thought as a 2D random field. Random variable set  $X = \{X_s, s \in S\}$ , it presumes that  $x_s$  is the realization of  $X_s$ . Pixel  $S$ 's the neighborhood is  $N_s$  and meets the conditions of probability distribution as follows:

$$P(X_s = x_s) > 0$$

$$P(X_s = x_s | X_r = x_r, r \in S, r \neq s) = P(X_s = x_s | X_r = x_r, r \in N_s)$$

We call that  $X$  is Markov random field (Lu Mingjun and Ruisheng, 2000; Jeng and Woods, 1991) with neighborhood  $N_s$ . Gibbs distribution keeps a close relationship with MRF. Gibbs distribution with neighborhood  $N_s$  is expressed in Eq. (6):

$$P(X = x) = \frac{1}{Z} e^{-U(x)} \quad (6)$$

where,  $U(x)$  is the energy function and represents as shown in Eq. (7):

$$U(x) = -\sum_{c \in C} V_c(x) \quad (7)$$

For Eq. (7),  $C$  is the set of cliques included by neighborhood  $N_s$  and  $V_c(x)$  represents the potential function of clique and  $Z = \sum_x e^{-U(x)}$  is the partition function. For the model base on MRF, the second order neighborhood specifies some parameters. Then, we can define the corresponding potential function as follows:

$$V_c(x) = \begin{cases} +\lambda, & \text{if pixel value is same} \\ 0, & \text{otherwise} \end{cases} \quad (8)$$

where,  $\lambda$  represents clique parameter.

**A blur parameter model based MRF:** Let  $X$  denotes the random fields corresponding to the blur parameter  $\rho^j$ ,  $X$  can be modeled by MRF. Namely, it shows as in Eq. (9):

$$P(X = x) = \frac{1}{Z} e^{-U(x)} \quad (9)$$

If  $Y_1, Y_2$  denote the random fields corresponding to the two observed images, the posterior probability can be expressed as Eq. (10):

$$P(X | Y_1, Y_2) = \frac{P(Y_1, Y_2 | X)P(X)}{P(Y_1, Y_2)} \quad (10)$$

where,  $P(Y_1, Y_2)$  is a constant and  $P(X)$  is the previous probability of the blur parameter.  $P(X|Y_1, Y_2)$  is the posterior probability of the initial image, with knowing  $Y$  value. So, according to Bayes rules, the depth restoration of the defocus image can be converted into the problem that seeks the estimation of the original image when the posterior probability is maximization. Surely, there are two main problems we have deal with: (1) computes the previous probability; (2) computes the maximization posteriori probability (MAP). Now, we give the implementation above two problems, respectively.

**IMPLEMENTATION**

**The previous probability computation:** Given X as the blur parameter of the defocus image, Let thinks X as a MRF, the previous probability P(X) can be used Gibbs distribution to descript:

$$P(X) = \frac{1}{Z} \left[ e^{\sum_{c \in C} V_c(x)} \right] \quad (11)$$

For given the observed images  $y_1, y_2$ ,  $P(Y_1 = y_1, Y_2 = y_2)$  is a constant. Considering the observation model given by Eq. (12):

$$y_k(i, j) = h_k(i, j) * f(i, j) + w_k \quad k=1, 2 \quad (12)$$

where,  $f(i, j)$  is the clear focus image,  $y_k(i, j)$  is the blur defocus image,  $h(i, j)$  is the point spread function (PSF),  $w_k$  is the observed noise.  $h(i, j)$  has a relation corresponding to the blur radius. Following, we assume the observations of the MRF image  $y_s$  obeys the model in Eq. (13):

$$y_s = f(x_s) + w_s \quad (13)$$

where,  $f(x)$  is a function that maps  $x_s$  to  $\mu_s$ , and  $w_s$  are independently distributed Guassian random vectors with zero mean and unknown covariance matrix  $\Theta_{x_s}$ . The PSF  $h(i, j)$  is Gaussian with blur parameter. Hence, the probability  $P(Y_1 = y_1, Y_2 = y_2 | X)$  can be descript as Gaussian distribution and be shown as (14):

$$P(Y_1 = y_1, Y_2 = y_2 | X) = e^{-\sum_{s=1}^n \frac{1}{2\sigma^2} (y_1 - \mu_s)^2 - \sum_{s=1}^n \frac{1}{2\sigma^2} (y_2 - \mu_s)^2} \quad (14)$$

Then, formula (10) can be converted into (15):

$$P(X | Y_1 = y_1, Y_2 = y_2) = \frac{1}{Z} e^{\sum_{c \in C} V_c(x) - \sum_{s=1}^n \frac{1}{2\sigma^2} (y_1 - \mu_s)^2 - \sum_{s=1}^n \frac{1}{2\sigma^2} (y_2 - \mu_s)^2} \quad (15)$$

Based on the observed image  $y_1, y_2$ , the problem of depth estimation is to find the estimation  $\hat{x}$  of X, which can computes the depth indirectly.

**Improved ICM algorithm implementation:** Base on discussion above, the posterior probability  $P(X | Y_1, Y_2)$  about the original image can be converted into the optimization problem as shown in Eq. (16):

$$\min \left[ \sum_{c \in C} V_c(x) + \sum_s \frac{1}{2\sigma^2} (y_1 - \mu_s)^2 + \sum_s \frac{1}{2\sigma^2} (y_2 - \mu_s)^2 \right] \quad (16)$$

Now we employ Besag's Iterated Conditional Modes algorithm to complete the optimization problem. ICM

algorithm has a highest efficiency and reliable performance (Jaehyun and Kurz, 1996; Jong *et al.*, 1996). Compared with simulation annealing algorithm applying condition distribution to extract X, ICM algorithm searches condition distribution X when it is maximization. Note that, when each pixel has a few neighbours, this class is highly restricted by unobvious consistency conditions, it is necessary to preserve symmetry in naming neighbours: that is, if j is a neighbour of i then i must be a neighbour of j. As a result, we meet the conditions which ignores the large scale deficiencies of  $p(x)$  and selects a reasonable initial point to achieve a satisfactory result.

Besag (1986) suggestion for initial parameter estimation adopts Maximum Likelihood Estimation (MLE). The MLE method has many large sample properties that make it attractive for use. It is asymptotically consistent, which means that as the sample size gets larger, the estimates converge to the right values. It is asymptotically efficient, which means that for large samples, it produces the most precise estimates. It is asymptotically unbiased, which means that for large samples one expects to get the right value on average. Unfortunately, the size of the sample necessary to achieve these properties can be quite large: Thirty to fifty to more than a hundred exact failure times, depending on the application. With fewer points, the methods can be badly biased.

The least squares estimation method is quite good for functions that can be linearized. The calculations are relatively easy and straightforward, having closed-form solutions which can readily yield an answer without having to resort to numerical techniques or Tables. Further, this technique provides a good measure of the goodness-of-fit of the chosen distribution in the correlation coefficient. Least squares is generally best used with data sets containing complete data, that is, data consisting only of single times-to-failure with no censored or interval data. Therefore, The choice of initial point is employed Least Squares Estimate (LSE) to complete.

**Least squares estimate of initial parameters:** The conditional distribution is given in Eq. (15) and the observations of the MRF obeys the model in Eq. (13). Choose parameter estimates to minimize sum of squared errors:

$$N(\mu_s) = \sum_{s=1}^n (y_s - \mu_s)^2 \quad (17)$$

Differential with respect to parameter and set to 0 to get least squares estimates:

$$\frac{\partial N}{\partial \mu_s} = -2 \sum_{s=1}^n (y_s - \mu_s) = 0 \quad (18)$$

Then, the LSE are:

$$u_{x_s}^{\wedge} = \frac{1}{n} \sum_{s} y_{x_s} \quad (19)$$

$$\Theta_{x_s}^{\wedge} = \frac{1}{M^2} \sum_{\Omega} (y - \mu_{x_s}^{\wedge})^2 \quad (20)$$

where,  $\Omega$  is the complete set of  $M^2$  pixels. We use Eq. (19) and (20) as the initial point of the ICM algorithm.

**Steps of improved ICM algorithm:** The steps of improved ICM algorithm as follows:

- Step 1:** Obtain an initial estimate  $\hat{x}$  of the true  $x$ , with guesses for  $\delta$
- Step 2:** Estimate  $\delta$  by the value  $\hat{\delta}$  which maximizes  $P(y_1, y_2 | \hat{x}; \delta)$
- Step 3:** Carry out a single cycle of ICM (Step five to Step seven) based on the current  $\hat{x}$  and  $\hat{\delta}$  to obtain a new  $\hat{x}$
- Step 4:** Return to 2 for a fixed number of cycles or until computes repeat up to convergence
- Step 5:** (a single cycle of ICM) Given  $\hat{x}$  denotes a estimate of the true scene  $x^*$
- Step 6:** Obtain a new  $\hat{x}_i$  and use it to maximizes  $P(y_{1i}, y_{2i} | x_i)$  at each  $i$
- Step 7:** Judge if the number of cycles is arrived or not

### EXPERIMENTS

Microscopic visual servoing is the sensor-based control strategy in micro-assembly. The microscopic vision feedback has been identified as one of the more promising approaches to improve the precision and efficiency of micromanipulation tasks. Micromanipulation robotic system includes 3D micro-move platform (three micro manipulation hands), micro-gripper driven by piezoelectricity, micro-adsorption hand driven by vacuum, microscope vision and so on, which microscope vision includes stereo microscope with variable times panasonic CCD camera, Tianmin SDK2000 image capture board. The captured image in visual system is  $640 \times 480$  pixels.

Firstly, we construct the restoration model of the microscope vision defocus image based on MRF the same as (14). Presumes that the observed images are  $y_1, y_2$  and defines  $Y$  as the restoration image.  $Y$  is thought as a MRF. Then, we can restore the defocus image similarly as (14). During micromanipulation experiments, presumes the microscope work distances (the distances from object lens to clear imaging plane.)  $u_0 = 80$  mm and gives that micro-move platform zero point corresponding micro-effector tip position as original point in coordinate. Then, we revise microscope vision system in order to locate original point in clear imaging plane.

Figure 2 and 3 show the initial defocus image of micromanipulator with different camera setting. Figure 4 gives the restoration image of micromanipulator.

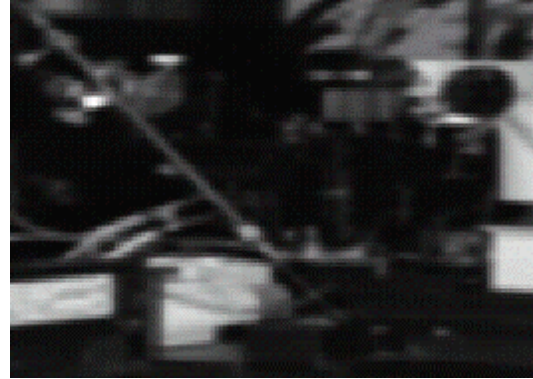


Fig. 2: The initial image of defocus image of micromanipulator

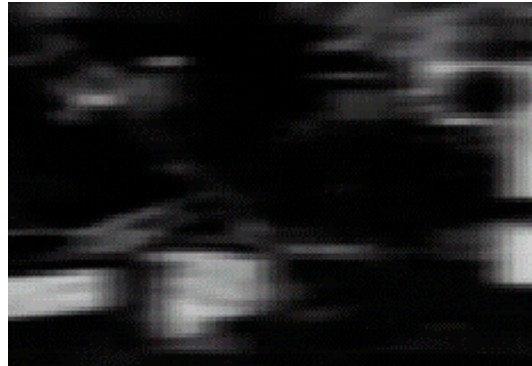


Fig. 3: The initial image of defocus image of micromanipulator with different camera setting



Fig. 4: The restoration image of defocus image of micromanipulator

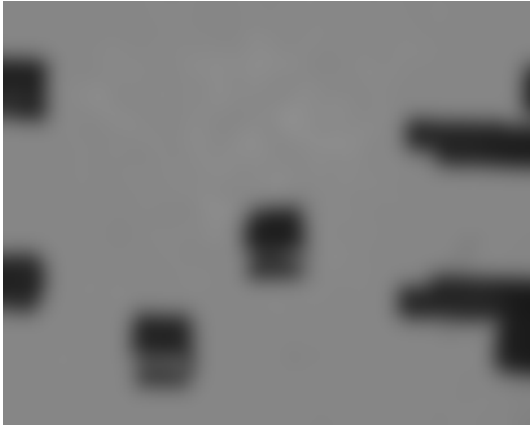


Fig. 5: The original defocus image of micro-gripper and metal cylinder with the blur  $\rho^1$



Fig. 7: The estimated value of the depth obtained using DFD with random the initial point

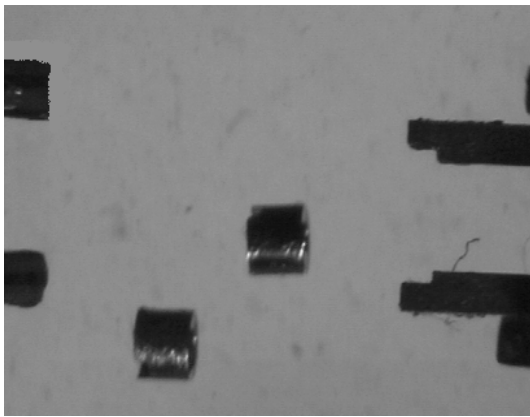


Fig. 6: The original defocus image of micro-gripper and metal cylinder with the blur  $\rho^2$

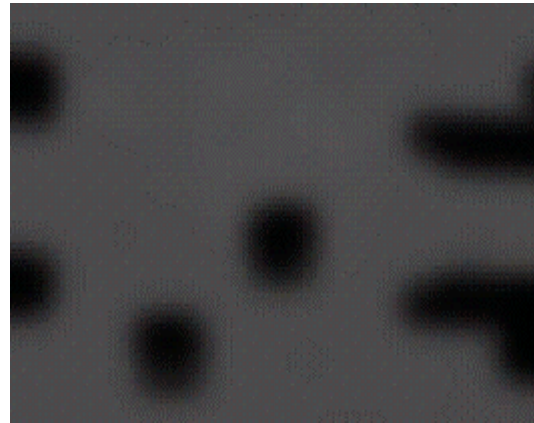


Fig. 8: The estimated value of the depth obtained using proposed method

Secondly, we give the performance of estimation of depth method. The image is magnified using the Taike XSZ monocular optics microscope (0.7-4.5x) and is captured by Panasonic WV-CP450 CCD camera with focus length of 2.5 cm. The lens aperture was kept constant at an f-number of 6. Two defocused images of the scene are taken for two different focusing ranges of 70 and 98 cm, which the nearest and the farthest points were at a distance of 80 and 100 cm from the camera to the object.

We demonstrate the performance of the method in estimating blur parameter and recovering the depth. The method of Subbarao (Subbarao, 2002) is employed to obtain initial estimates of  $\rho$ . We choose  $\rho_{ij}^2 = 0.4 \rho_{ij}^1$  and the number of level for the blur parameter is 30. The original defocus image with blur  $\rho^1$  and blur  $\rho^2$  is shown in Fig. 5 and 6, respectively. Figure 7 shows the estimated

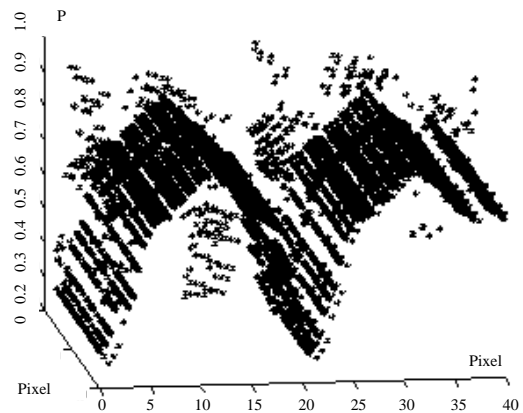


Fig. 9: The estimated values of the blur parameter using proposed method

value of depth obtained using DFD, which the initial point is given randomly (according to equation of the blur parameter). Correspondingly, the estimated value of the depth employed the proposed method that the initial point is chose using LSE is shown in Fig. 8. Figure 9 shows the estimated value of the blur parameter using the proposed method. From Fig. 8 and 9, compared with DFD that the initial point is given randomly, we note that the planar nature of the variation in the depth of the scene is better brought by the proposed method.

### CONCLUSION

The depth estimation in micromanipulation tasks is a key technology in microscope vision system. For the depth estimation of microscope vision image, This study presents a blur parameter model of the defocus image based on MRF. It converts problem of depth estimation into optimization problem. An improved Iterated Conditional Modes Algorithm has been applied to complete optimization problem, which prevents that performance result gets into local optimization. The experiments and simulations prove that the model and algorithm is efficiency. It provides the probability that finishes visual servoing control in 3D space.

### REFERENCES

Besag, 1986. On the statistical analysis of Dirty Pictures. *J. R. Stat. Soc. Series B*, 48: 259-302.  
Deschenes, F., D. Ziou and P. Fuchs, 2004. An unified approach for a simultaneous and cooperative estimation of defocus. *Image Vision Comput.*, 22: 35-57.

Djemel, Z. and F. Deschenes, 2001. Depth from defocus estimation in spatial domain. *Comput. Vision Image Understanding*, 81: 143-165.  
Du Ming, T.S.A.I. and C.T. Lin, 1998. A moment preserving approach for depth from defocus. *Pattern Recognition*, 31: 551-560.  
Jaehyun, P. and L. Kurz, 1996. Image enhancement using the modified ICM method. *IEEE. Trans. Image Processing*, 15: 765-771.  
Jeng, F. and J. Woods, 1991. Compound Gauss random fields for image estimation. *IEEE. Trans. Signal Processing*, 39: 683-691.  
Jong, K.F., Petar and M. Djuric, 1996. Unsupervised vector image segmentation by a trss structure-ICM algorithm. *IEEE. Trans. Med. Imaging*, 15: 871-880.  
Lu Mingjun and W. Ruisheng, 2000. A markov random field method in computer vision. *J. Elect. Sci.*, 22: 1028-1037.  
Rajagopalan, A.N. and S. Chaudhuri, 1999. An MRF model based approach to simultaneous recovery of depth and restoration form defocused images *IEEE. Trans. Pattern Anal. Mach. Intell.*, 21: 577-589.  
Soon, Y.P., 2006. An image based calibration technique of spatial domain depth from defocus. *Pattern Recognition Lett.*, 27: 1318-1324.  
Subbarao, M., 2002. Parallel depth recovery by changing camera parameters. *Proceedings of the IEEE Conference on Computer Vision*, Dec. 5-8, IEEE Xplore London, pp: 149-155.  
Vinay, P.N. and S. Chaudhuri, 2007. On defocus, diffusion and depth estimation. *Pattern Recognition Lett.*, 28: 311-319.